Water Practice & Technology

IWA PUBLISHING

Water Practice & Technology Vol 18 No 1, 140 doi: 10.2166/wpt.2022.154

Modelling and optimization of energy consumption in the activated sludge biological aeration unit

Mpho Muloiwa[a,*], M. O. Dinka[b] and Stephen Nyende-Byakika[a]

[a] Department of Civil Engineering, Tshwane University of Technology, Private Bag X680 Pretoria 0001, Staatsartillerie Road, Pretoria West, South Africa
[b] Department of Civil Engineering Science, University of Johannesburg, Auckland Park Campus 2006, Box 524, Johannesburg, South Africa
*Corresponding author. E-mail: muloiwam@yahoo.com

ABSTRACT

The biological aeration unit consumes the highest energy (67.3%) in wastewater treatment compared with physical (18.8%) and chemical (13.9%) treatment processes. The high energy consumption is caused by the supply of oxygen using air pumps/blowers and temperature that controls microorganisms' growth. The purpose of this study was to model and optimize energy consumption in the biological aeration unit. The multilayer perceptron (MLP) artificial neural network (ANN) algorithm was used to model energy consumption. The particle swarm optimization (PSO) algorithm was used to optimize the energy consumption model. Sensitivity analysis was performed to determine the percentage contribution of input variables towards energy consumption. The MLP ANN algorithm modelled energy consumption successfully and produced R^2, RMSE, and MSE of 0.89, 0.0265, and 0.00070, respectively, during the testing phase. The PSO algorithm optimized energy consumption successfully and produced a global solution of 0.993 kWh/m^3. The percentage reduction between the lowest measured and optimized energy consumption was 38.4%. Aeration period (81%) and temperature (10.7%) contributed the highest towards energy consumption. In conclusion, temperature played a significant role in energy consumption compared with airflow rate (4.2%). When the temperature is conducive to allowing the growth of microorganisms, the removal of COD and ammonia will be rapid resulting in low energy consumption.

Key words: artificial neural network, biological aeration unit, energy consumption, modelling, particle swarm optimization, wastewater treatment plant

HIGHLIGHTS

- Temperature is the driver of energy consumption compared with airflow rate in the biological aeration unit.
- Temperature contributes 6.5% more than airflow rate towards energy consumption in the biological aeration unit.
- Biological aeration unit should be operated at high temperatures (35 °C) in order to achieve low energy consumption.
- A total of 38.4% reduction in energy consumption was achieved using the PSO algorithm.

GRAPHICAL ABSTRACT

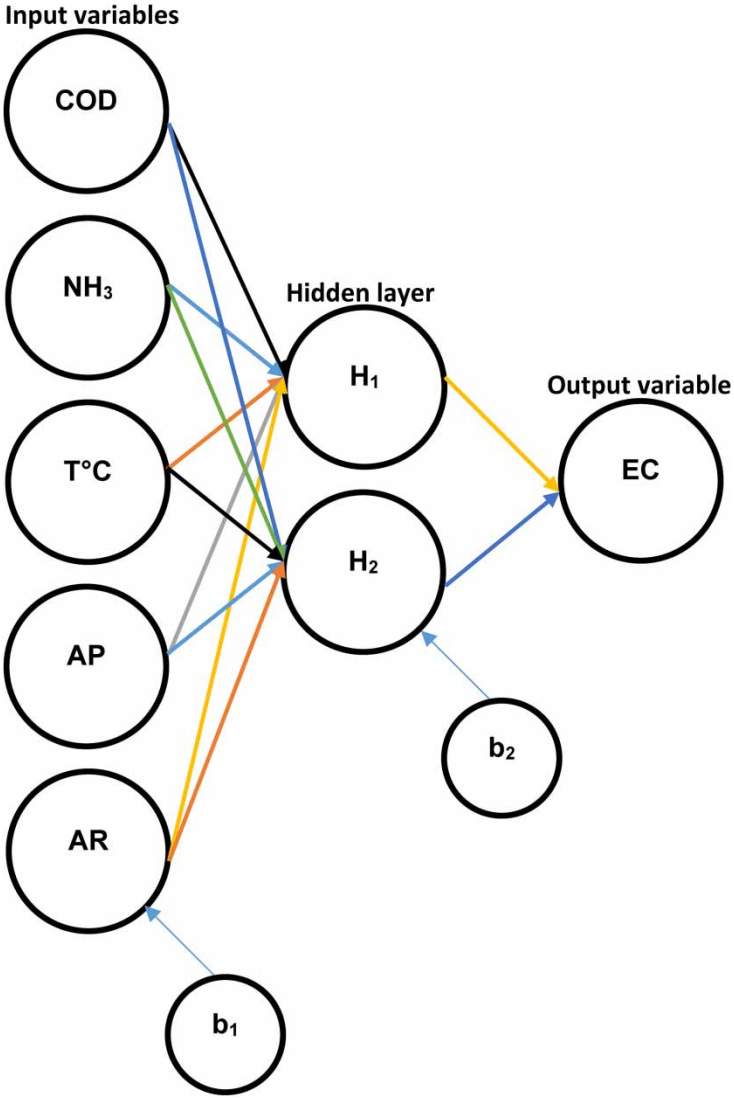

1. INTRODUCTION

Wastewater treatment plants (WWTPs) are used all over the world including South Africa (SA). WWTPs are responsible for treating domestic and industrial wastewater to an acceptable effluent quality before being discharged into the environment (Żyłka *et al.* 2021). Treatment of wastewater is achieved using different treatment processes such as physical, biological, and chemical (Crini & Lichtfouse 2019). The physical treatment process is mainly responsible for removing large objects using physical methods such as screens and sedimentation tanks (Saleh *et al.* 2020). The biological treatment process is responsible for decomposing organic matter and oxidizing inorganic matter using microorganisms (Kanaujiya *et al.* 2019). The chemical treatment process is usually the final step responsible for chemical stabilization and disinfection of the wastewater before it is discharged into the environment (Singh 2022). WWTPs consume energy during each of the treatment processes in attempting to meet the desired effluent discharge quality (Musvoto & Ikumi 2016).

In SA, physical treatment processes consume on average 0.148 kWh/m³, which is about 18.8% of the total energy consumed by a WWTP (Winter 2011; Van Vuuren 2013; Musvoto & Ikumi 2016). In Italy and Australia, energy consumption was reported to be 0.113 and 0.37 kWh/m³ for the physical treatment process, respectively (Panepinto *et al.* 2016; Wakeel *et al.* 2016). The biological treatment process consumes the highest energy in a WWTP (Baquero-Rodríguez *et al.* 2022). In SA, the biological treatment process consumes 0.53 kWh/m³, which amounts to 67.3% of the total energy consumed in a WWTP (Winter 2011; Van Vuuren 2013; Musvoto

& Ikumi 2016). In Spain and Saudi Arabia, the biological treatment process consumes 0.8 and 1.6 kWh/m³, respectively. The chemical treatment process amounts to 13.9% of the total energy consumed in a WWTP. In the United States of America (USA) and Japan, the chemical treatment process consumes on average 0.23 and 0.39 kWh/m³, respectively (Stasinakis *et al*. 2022).

Research has shown that the biggest driver of energy consumption in the biological aeration unit is the airflow supply (Wakeel *et al*. 2016; Li *et al*. 2017; Singh & Kansal 2018; Christoforidou *et al*. 2020; Siatou *et al*. 2020). Airflow supplies the oxygen required by microorganisms for respiration in the biological aeration unit (Vogelaar *et al*. 2000). High airflow rates produce sufficient dissolved oxygen (DO) required by microorganisms, however high airflow rates consume high energy due to large air pumps/blowers utilized (Chiavola *et al*. 2017). Because of the impact of high airflow supply in the biological aeration unit, different scholars were encouraged to develop optimization models that were focused on optimizing the airflow supply since it was reported to be the biggest driver of energy consumption (Kusiak & Wei 2013; Ozturk *et al*. 2016; Asadi *et al*. 2017; Chiavola *et al*. 2017; Han *et al*. 2018; Huang *et al*. 2019; Lu *et al*. 2021).

Ozturk *et al*. (2016) optimized energy consumption by minimizing the aeration rate in the biological aeration unit. The results reduced the airflow rate by 72%, resulting in less energy consumption. Asadi *et al*. (2017) optimized the biological aeration unit by developing a model that minimizes DO concentration. The results showed that the airflow rate was optimized by 31%, resulting in low energy consumption. Chiavola *et al*. (2017) optimized the biological aeration unit energy consumption by reducing DO concentration to 2 mg/l. The results of the study achieved a 13% reduction in energy consumption. Kusiak & Wei (2013) applied the PSO algorithm in attempts to optimize energy consumption in the activated sludge process. The results of the study showed that a 15% airflow rate reduction minimized energy consumption. The literature detailed above shows that all authors focused on reducing airflow supply into the biological aeration unit. This allowed for a reduction in energy consumption in the biological aeration unit.

Although the reduction of energy consumption was achieved by reducing airflow supply into the biological aeration unit, the current study will show that temperature plays a vital role in reducing energy consumption in the biological aeration unit. This is because microorganisms require a conducive environment for survival, and if the environment is not conducive, longer aeration periods will be required (Loutfi *et al*. 2020). Temperature controls the environment that allows the growth of microorganisms and enhances the metabolic rate in the biological aeration unit (Chapra *et al*. 2021). Microorganisms commonly found in wastewater are classified as mesophilic and they grow in the temperature range between 10 and 45 °C, with an optimum of 32.5 °C (Brandam *et al*. 2008; Zeraik & Nitschke 2012; Haberl-Meglič *et al*. 2016; Menegol *et al*. 2017; Balku 2018; Pawlita-Posmyk *et al*. 2018; Brehar *et al*. 2019; Shen *et al*. 2020). For example, Balku (2018) reported that biomass concentrations of 1,550.1; 1,474.4; 1,346.9; 1,188.2 g/m³ were measured at temperatures of 30, 20, 10, and 0 °C, respectively. Shen *et al*. (2020), reported that a temperature of 33 °C produced a biomass concentration of 0.6 g/l, and a temperature of 25 °C produced biomass of 0.2 g/l. Therefore, low temperatures (18–22 °C) will slow down the growth of microorganisms, and as a result extended aeration period will be required, which results in high energy consumption (Drewnowski *et al*. 2019). However, if the temperature in the biological aeration unit is maintained at 32.5 °C, the growth of microorganisms will be at an optimum, resulting in rapid removal of chemical oxygen demand (COD) and ammonia. This means that less airflow supply and aeration period will be required, resulting in low energy consumption. The current research will close this existing research gap. The aim of the study was to apply artificial neural network (ANN) and particle swarm optimization (PSO) algorithms in attempts to model and optimize energy consumption in the biological aeration unit. The optimization model will in cooperate for the first time temperature and airflow supply because they are the biggest drivers of energy consumption in the biological aeration unit.

2. MATERIALS AND METHODS

2.1. Laboratory experiments

Laboratory experiments were carried out to simulate energy consumption during COD and ammonia removal at different airflow rates and wastewater temperatures. The airflow rates used were 5, 10, 15, 20, 25, and 30 l/min. The temperatures used were 15, 17.5, 20, 22.5, 25, 27.5, 30, 32.5, and 35 °C. Aeration was performed for 4 h nonstop and samples were taken every 2 h. Samples taken were initial concentration, 2-h mark concentration, and 4-h mark concentration, which resulted in three samples per event. Each sample was examined twice in

order to check the consistency of the results. The total data points collected were 324. Laboratory data were analyzed using a correlation matrix and linear regression. The biological aeration unit components and the schematic diagram are detailed in Table 1 and Figure 1, respectively.

Table 1 | Components of the aeration unit

Components	Type	Remarks
Aeration tank	Circular aeration tank. (acrylic material)	10–15 mm thick Acrylic material. Dimensions 570 × 300 mm. Total volume is 40 l. Working volume is 30 l
Dissolved oxygen meter and probe	Hanna HI98196 multi-parameter water proof meter	Measures DO, pH, and ORP
Thermostat	Local manufacturer	Controls temperature in the range 0–40 °C
Air pump	Waterfall Resun LP100	Can supply air between 0 and 140 l/min
Airflow meter	MF5712 200 l/min digital gas air nitrogen oxygen mass flow meter	Can measure airflow rate between 0 and 200 l/min
Air stone disc bubble diffuser	Growneer micro pore bubble diffuser	Diffuser is 20 cm in diameter
Digital wattmeter	Geewiz (Kill a watt)	Measures power between 0 and 3,600 W

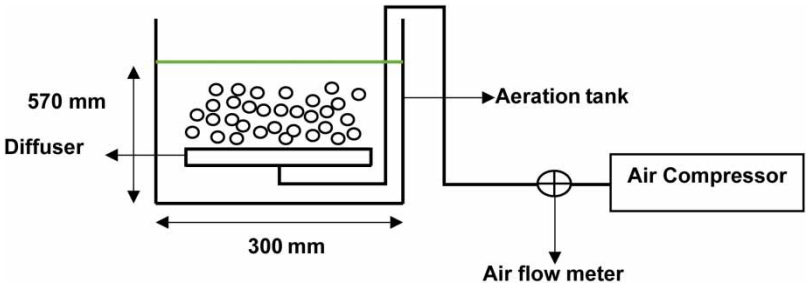

Figure 1 | Laboratory aeration unit.

2.2. Wastewater collection, disposal, and analysis

The APHA (2012) method was used for the collection of wastewater from the WWTP. Wastewater was collected at the Daspoort WWTP, Pretoria, Gauteng Province, South Africa, coordinates (−25.733857, 28.177894). The Daspoort WWTP consists of three bioreactors, and the samples were collected from reactor number two. Non-sterile powder-free nitrile gloves were used to handle all equipment. A 25-l jerry was used to collect the raw wastewater. An additional 2 l of activated sludge was collected from the return activated sludge. Wastewater samples were collected and aerated within 8 h after collection. After the completion of the aeration process, wastewater was disposed by flushing at the laboratory toilet. The disposal method allowed the wastewater to go back to the WWTP. Two wastewater characteristics were measured, namely COD and ammonia (NH_3). The method used for analyzing wastewater characteristics was the Standard Methods for the Examination of water and wastewater (APHA 2012). Table 2 provides the details on the wastewater characteristics analysis.

Table 2 | Analysis of wastewater characteristics

Parameter	Equipment	Method
COD	Spectrophotometer closed reflux colorimetric, Digestion vessels, Block heater, Microburet, and Ampule sealer. DR3900	APHA (2012) method 5220
Ammonia	Spectrophotometer and reagents were used. DR3900	APHA (2012) method 4500

2.3. Energy consumption

Energy consumption was measured in kilowatt-hour (kWh), and then later expressed in terms of the total energy consumed per volume of wastewater treated (kWh/m³). The power output of the air pump was measured using a digital plug-and-play wattmeter as described in Table 1. The digital wattmeter is also equipped with a timer, which was used to monitor the aeration period. Energy consumption was analyzed using the correlation coefficient. The correlation coefficient was conducted on Statistical Package for the Social Sciences Software (SPSS) version 27.

2.4. Application of ANN

A regression model was developed using the multilayer perceptron (MLP) ANN algorithm on MATLAB programming software. Continuous data collected from laboratory experiments were used to develop the energy consumption model. Eight steps were followed to model energy consumption using the MLP ANN algorithm.

- The first step was to select input variables from the data collected during laboratory experiments.
- The second step was to split the data into 70% training, 15% validation, and 15% testing.
- The third step was to transform data into input variables using the normalization technique defined by Equation (1).

$$x(\text{scaled}) = \frac{x - \min_x}{\max_x - \min_x} \tag{1}$$

where x(scaled) is the scaled sample data point, x is the sample data point, $\min_x$ is the minimum value in the training dataset, $\max_x$ is the maximum value in the training dataset.

- The fourth step was to select the MLP ANN architecture with one hidden layer and two neurons.
- The fifth step was to initialize the weights and bias between values of 0 and 1.
- The sixth step was to use the sigmoid activation function as a transfer function. The sigmoid function is defined by Equation (2) and Figure 2.

$$f = \frac{1}{1 + e^{-x}} \tag{2}$$

- The seventh step was to use the supervised gradient descent backpropagation learning algorithm to correct the weights and bias.
- The eighth step was to evaluate the performance of the energy consumption model using MSE, R^2, and RMSE defined by Equations (3)–(5),respectively.

$$MSE = \sum_{i=1}^{n} \frac{(\hat{y}_i - y_i)^2}{N} \tag{3}$$

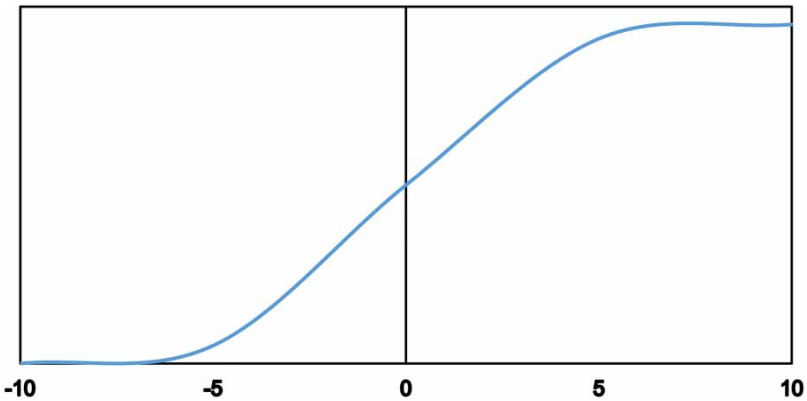

Figure 2 | Sigmoid function.

$$R^2 = \frac{1}{m}\sum_{j=1}^{m}\left(1 - \frac{SSE}{SST}\right) \tag{4}$$

$$RMSE = \sqrt{\frac{\sum_{i=1}^{n}(\hat{y}_i - y_i)^2}{N}} \tag{5}$$

where MSE is the mean squared error, $\hat{y}_i$ is the predicted value, y_i is the observed value, N is the number of data points, R^2 is the coefficient of determination, SSE is the sum of squared error, and SST is the total sum of squares.

2.5. Application of the PSO algorithm

Ten steps were followed to apply the PSO algorithm.

- Step 1 was to initialize the number of particles to 30.
- Step 2 was to initialize the random numbers r_1 and r_2 to 1.
- Step 3 was to initialize the acceleration constants c_1 and c_2 to 1.
- Step 4 was to initialize the initial velocity of each particle to 0.
- Step 5 was to initialize the initial position of each particle randomly in the search space.
- Step 6 was to update each particle's velocity, personal best position of each particle, and global best of the population using Equations (6) and (7).

$$x_{ij}(t+1) = x_{ij}(t) + v_{ij}(t+1) \tag{6}$$

$$v_{ij}(t+1) = w \times v_{ij}(t) + c_1 \times r_1(p\text{best}_{i,j} - x_{i,j}(t)) + c_2 \times r_2(g\text{best}_j - x_{i,j}(t)) \tag{7}$$

- Step 7 was to select the personal best position of each particle by comparing it with the new position at which the particle has landed on/travelled to.
- Step 8 was to select the global best position from the personal best position of each particle.
- Step 9 was to repeat steps 6, 7, and 8 until convergence has been reached in the search space. The pseudo code used is shown in Table 3.
- Step 10 was to conduct sensitivity analysis on the decision variables that contribute most to the optimization results. A one-factor-at-a-time method was used. Each decision variable was individually adjusted by ± 10, ± 20, and $\pm 50\%$, while keeping the others unchanged. In addition, decision variables were checked for their direct, inverse, major, or minor changes in energy consumption. The observed versus the optimized energy consumption data were analyzed using the ANOVA test.

Table 3 | Pseudo code for single objective problem

PSO algorithm
1. Initialize the particles' position (x^i), velocity (v^i), previous best position (p^i), and the number of particles N
2. While ($t <$ maximum number of iterations (T)) do
3. For all particles (i) do
4. Calculate the fitness function for the current position xi of the i^{th} particle ($F(x^i)$)
5. If ($F(x^i) < F(p^i)$) then
6. $P^i = x^i$ end if
7. If ($F(x^i) < F(G)$) then
8. $G = x^i$
9. End if
10. Adjust the velocity and positions of all particles according to Equations (1) and (2).
11. End for
12. Stop the algorithm if a sufficiently good fitness function is met
13. End while

3. RESULTS AND DISCUSSIONS

3.1. Analysis of laboratory results

Table 4 and Figures 3(a)–(e) present correlation matrix results and the graphic relationship between energy consumption and input parameters, respectively. The relationship between energy consumption and the aeration period produced a positive correlation of 0.920**. This means that when the aeration period was extended by 2 h, energy consumption also increased because the air pumps/blowers continued operating for longer periods of time. Most studies have recommended an aeration period of 4 h depending on the design of the WWTP (Bhargava 2016; Murillo 2018; Jasim 2020). The 4-h aeration period allows for the complete removal of COD and ammonia in wastewater. Hence, the correlation of COD (−0.860**) and ammonia (−0.759**) with the aeration period was negative as shown in Table 4. Figure 3(a) shows the graphic relationship between energy consumption and the aeration period. Figure 3(a) shows that at aeration period zero, energy consumption was also zero because there was no airflow supply. After 2 h of aeration, energy consumption was recorded to be in the range between 0.0435 and 0.086 kWh. After 4 h of aeration, energy consumption was recorded in the range between 0.087 and 0.172 kWh. This shows that extending the aeration period will result in high energy consumption because the airflow supply will continue in the biological aeration unit.

Table 4 | Correlation matrix between energy consumption and parameters

Correlations

		EC	AP	*T* (°C)	NH_3	COD	AR
EC	PC	1					
Time	PC	0.920**	1				
T (°C)	PC	0.000	0.000	1			
NH_3	PC	−0.689**	−0.759**	−0.392**	1		
COD	PC	−0.781**	−0.860**	−0.123**	0.712**	1	
AR	PC	0.337**	0.000	0.000	0.020	0.008	1

**Correlation is significant at the 0.01 level (two-tailed).

PC, Pearson correlation; EC, energy consumption; T, temperature; NH_3, ammonia; AR, airflow rate; AP, aeration period.

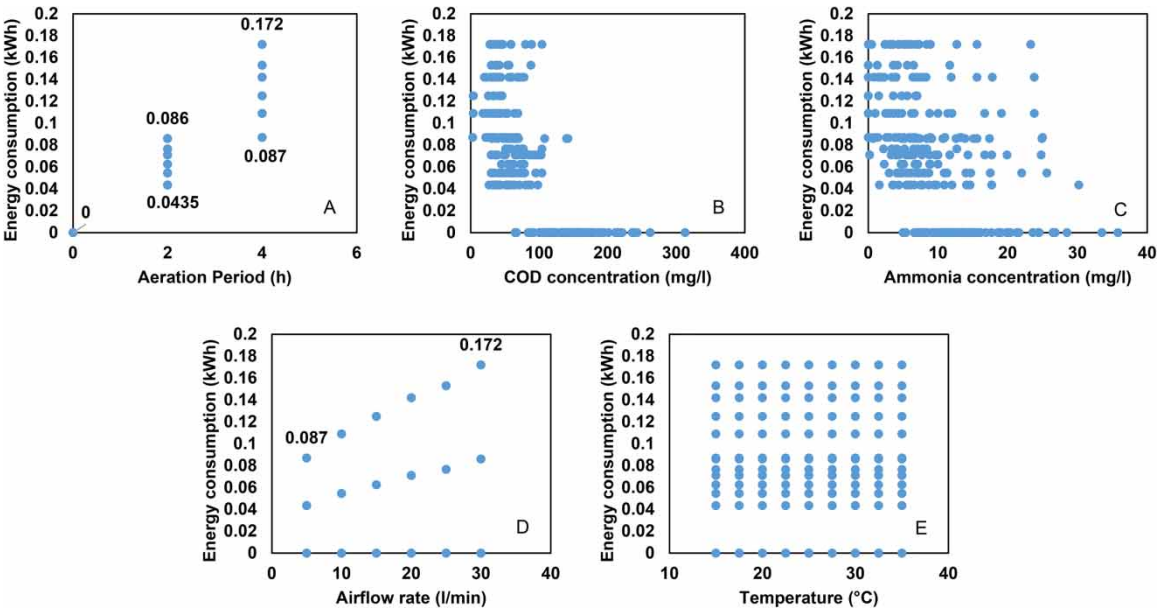

Figure 3 | Relationship between energy consumption and input variables: (a) Aeration period, (b) COD concentration, (c) ammonia concentration, (d) airflow rate, and (e) temperature.

Similar to the aeration period, the relationship between energy consumption and airflow rate produced a positive correlation of 0.337**. This indicates that when the airflow rate increased, energy consumption also increased because a higher demand of power was required from the air pumps/blowers. Energy consumption was expressed in terms of the air pump/blower power for every aeration period that the air pump/blower is utilized (kW h) (Guerrini *et al.* 2017; Singh & Kansal 2018). This means that when there is an increase in power demand (kW), energy consumption will increase in the biological aeration unit. Figure 3(d) shows the graphic relationship between energy consumption and airflow rate. In Figure 3(d), an airflow rate of 5 l/min resulted in an energy consumption of 0.087 kWh, and an airflow rate of 30 l/min resulted in energy consumption of 0.172 kWh. This implies that increasing the power demand will result in high energy consumption in the biological aeration unit.

The relationship between energy consumption and COD produced a negative correlation of −0.781** as shown in Table 4. This means that when COD is reduced to acceptable discharge standards, energy consumption increases. Energy consumption during COD removal is consumed indirectly. During COD removal, oxygen is essential for the respiration of microorganisms, and the oxygen is supplied using air pumps/blowers. Hence COD removal results in high energy consumption because air pumps/blowers supply oxygen (Dai *et al.* 2019; Siatou *et al.* 2020; Marlina *et al.* 2021). In addition, when COD removal takes time, the aeration period will increase resulting in high energy consumption. This can be justified by the relationship between COD and the aeration period which produced a negative correlation of −0.860**. This means that when there is an increase in the rapid removal of COD, less aeration period will be required, resulting in less energy consumption because air pumps/blowers will be utilized for a shorter period of time (Alisawi 2020; Amiri *et al.* 2020; Chakawa & Aziz 2021). Figure 3(b) shows the graphic relationship between energy consumption and COD removal. It can be observed in Figure 3(b) that high energy consumption was recorded at a low COD concentration, at the end of the aeration process. This means that in order to achieve low COD concentrations, large quantities of energy will be consumed.

The relationship between energy consumption and ammonia produced a negative correlation of −0.689**. Similar to COD removal, ammonia removal consumes energy indirectly. Energy consumption during ammonia removal is consumed similar to COD removal since ammonia removal relies on microorganisms (Jiang *et al.* 2018; Zou *et al.* 2019). Figure 3(c) shows the graphic relationship between energy consumption and ammonia removal. Similar to COD removal, high energy consumption was recorded at low ammonia concentration, at the end of the aeration process. This means that in order to achieve low ammonia concentrations, large quantities of energy will be consumed. The temperature was neither positively nor negatively correlated to energy consumption. However, temperature affects energy consumption indirectly because it controls the removal efficiency of COD and ammonia (Zhang *et al.* 2019; Alisawi 2020). At low temperatures, the growth and metabolic rate of microorganisms are low which results in a slow removal of COD and ammonia in wastewater. Alisawi (2020) reported COD removal of 40 and 70% were measured at temperatures of 10 and 30 °C, respectively. Zhang *et al.* (2019) reported the highest and lowest ammonia removal of 98 and 78% at temperatures of 18 and 13 °C, respectively. This indicates that when low temperatures are applied, a longer aeration period will be required in order to achieve acceptable discharge standards, which will result in high energy consumption. This can also be justified by the correlation of COD (−0.123**), and ammonia (−0.392**) on temperature shown in Table 4. The relationship between temperature, COD, and ammonia indicates that high temperatures will accelerate the removal of COD and ammonia, resulting in less aeration period required. Less aeration period means that less airflow supply will be required, therefore less energy will be consumed. Figure 3(e) presents the relationship between energy consumption and temperature.

3.2. Modelling energy consumption

The general form of the MLP ANN algorithm is shown in Equation (8). Where X is the jth nodal value for the previous layer. Y is the ith nodal value in the current layer. f is the activation function. W_{ij} is the weighting factor, and b is the bias of the ith node.

$$Y_i = f\left(\sum_{j=1}^{N} W_{ij}X_j + bi\right) \tag{8}$$

A total of five input variables were used as inputs to model energy consumption using MLP ANN algorithm. The input variables used were aeration period (AP), COD, ammonia, airflow rate (AR), and temperature (T °C). A total of 324 data points were used to train, validate, and test the model. The data were split into 70% training (226), 15% validation (49), and 15% testing (49). The MLP ANN network architecture is shown in Figure 4.

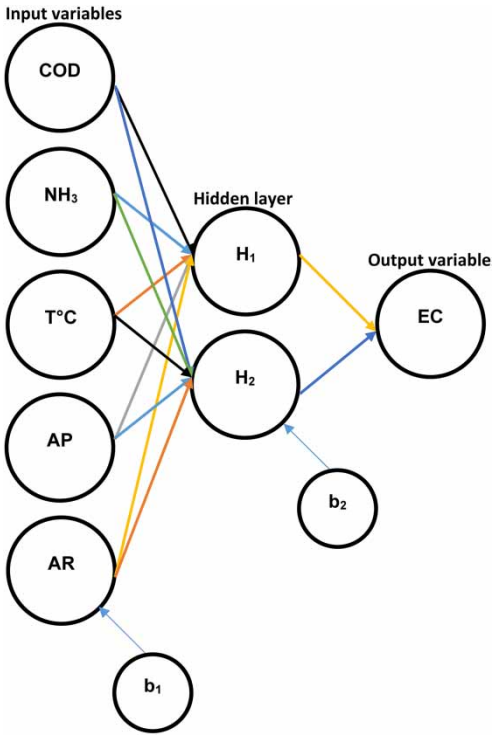

Figure 4 | MLP ANN energy consumption architecture.

Figure 5 shows the 226 observed energy consumption data that were used as input data during the training phase and the predicted energy consumption data from the MLP ANN energy consumption model during the training phase. The predicted data were close to the observed data, therefore MLP ANN algorithm was able to predict the energy consumption data during the training phase. Although the energy consumption model showed signs that it struggled to predict the high values, the overall performance of the model was acceptable.

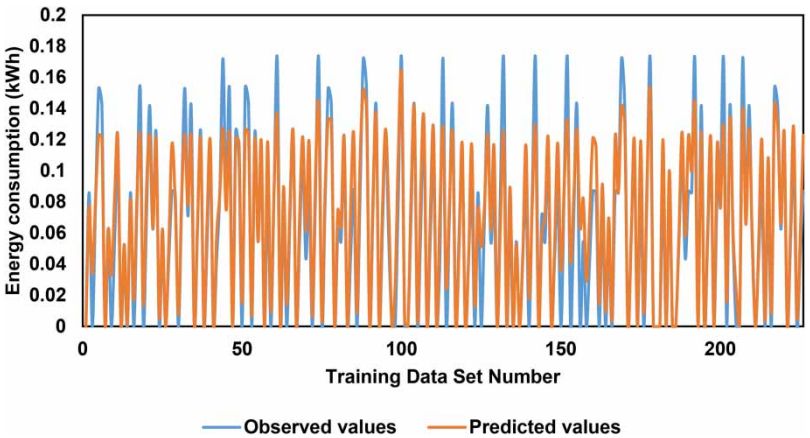

Figure 5 | Observed vs. predicted values during the training phase.

Figures 6 and 7 show the 49 observed data that were determined during the experiments and the predicted data from the MLP ANN algorithm during the validation and testing phase of the energy consumption model, respectively. During the validation phase, the model predicted the minimum, middle, and maximum values accurately compared with the training phase. This means that the model generalized the data accurately as shown in Figure 6. Similarly, the model was able to predict the observed data during the testing phase.

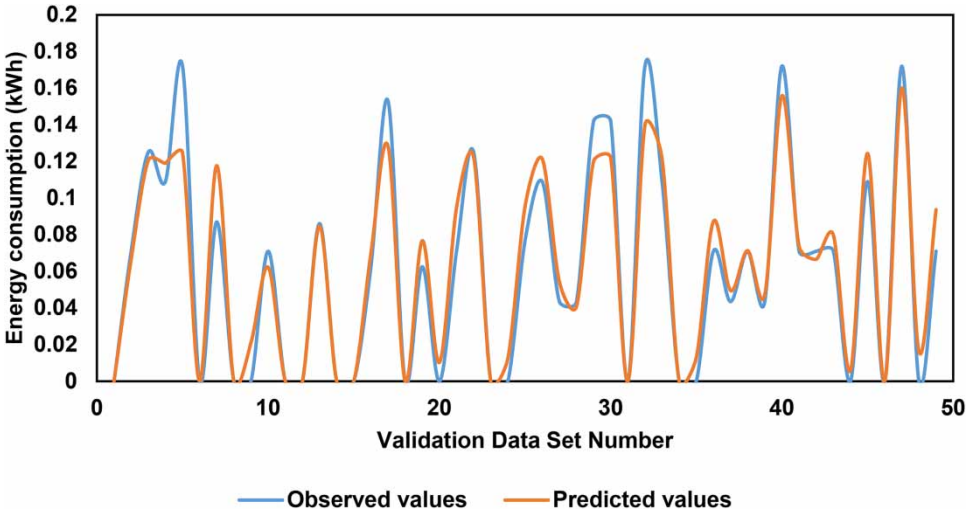

Figure 6 | Observed vs. predicted values during the validation phase.

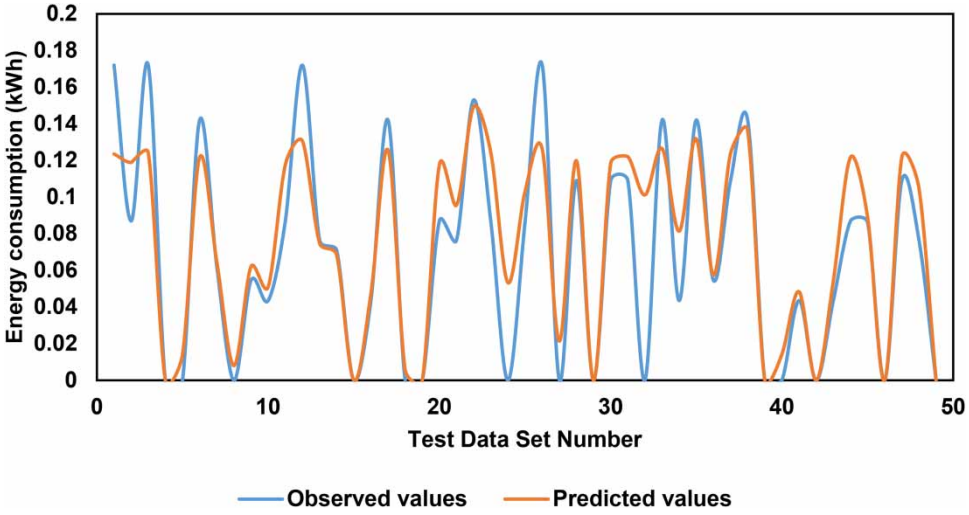

Figure 7 | Observed vs. predicted values during the testing phase.

The prediction accuracy of the MLP ANN energy consumption model was evaluated using R^2, RMSE, and MSE as shown in Table 5. The optimum MSE of 0.00026596 was determined during the validation phase of the energy consumption model. The highest MSE of 0.00070446 was determined during the testing phase of the model. Although the testing phase produced the lowest performance, the model performance was still acceptable. This means that the distance between the data points and the regression line is close to each other. The difference between the highest and lowest MSE was 62.25%, which was a significant difference. The MLP ANN energy consumption model performed well in all learning phases (training, validation, and testing).

The RMSE during training, validation, and testing phase results were 0.2, 0.016, and 0.0265, respectively, as shown in Table 5. The optimum RMSE was determined during the validation phase, which justifies that the

Table 5 | MLP ANN energy consumption model performance

	MSE	RMSE	R^2
Training	0.00040857	0.02	0.93
Validation	0.00026596	0.016	0.95
Testing	0.00070446	0.0265	0.89

optimum MSE was obtained during the validation phase. The difference between the highest and lowest RMSE was 39.6%, which was a significant difference. The R^2 also showed good performance during the training, validation, and testing phases. The training phase of the model produced R^2 value of 93.38% as shown in Figure 8(a). This means that 93.38% of the data points fit the model perfectly. Outlies are visible in Figure 8(a), which means that some of the data points did not fit the model perfectly during the training phase.

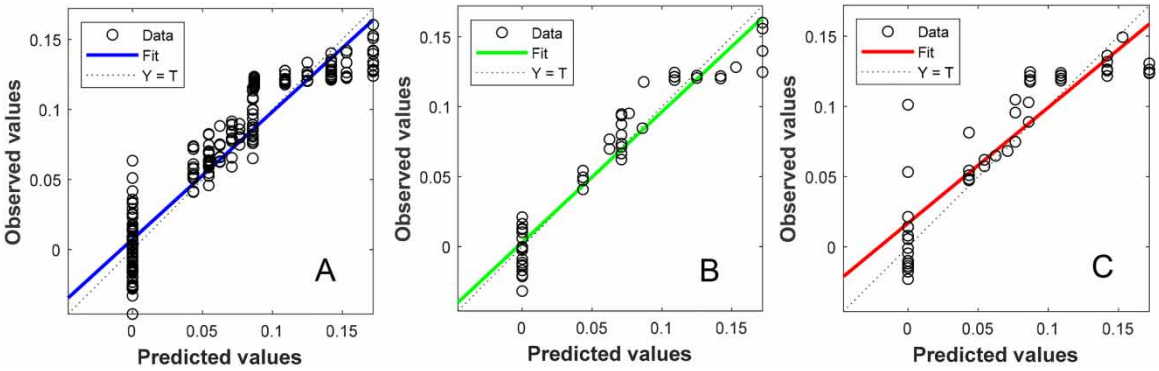

Figure 8 | (a) R^2 during the training phase, (b) validation phase, and (c) testing phase.

The validation phase produced R^2 value of 95.8% as shown in Figure 8(b). This means that 95.8% of the data points fit the model perfectly. Outliers were visible which means that some of the data points did not fit the model perfectly. The testing phase produced R^2 value of 89.1% as shown in Figure 8(c). This was a slight drop from the validation R^2. In other words, the model generalized the training dataset perfectly. There are fewer outliers compared with the validation phase, which shows that the model learned the training data perfectly.

The results obtained in this study were similar to results obtained from other studies (Güçlü & Dursun 2010; Hamada *et al.* 2018; Bekkari & Zeddouri 2019; Hassen & Asmare 2019; Sharghi *et al.* 2019; Struk-Sokołowska *et al.* 2019; Demir 2020; Newhart *et al.* 2020). Bekkari & Zeddouri (2019) reported that the ANN algorithm was successful with modelling the effluent COD, and produced R^2 value of 89, 96, and 87% during training, validation, and testing phases, respectively. MSE values of 0.007, 0.002, and 0.0045, respectively, and the results were similar to the results obtained in the current study. Güçlü & Dursun (2010) reported that the ANN algorithm produced R^2 value of 87 and 85% during training and testing phases, respectively, and the results were similar to the results obtained in the current study. Sharghi *et al.* (2019) reported that the ANN algorithm produced R^2 value of 74, 70, and 67% during training, validation, and testing phases. The results were in agreement with the results obtained in the current study.

Similarly, Hamada *et al.* (2018) reported that the ANN algorithm produced R^2 value of 82, 71, and 81% during training, validation, and testing phases, and the results were in agreement with the results obtained in the current study. Similarly, Demir (2020) reported that the ANN algorithm produced R^2 value of 98% and MSE of 0.000302, which were similar to results obtained in the current study. Struk-Sokołowska *et al.* (2019) reported that the ANN algorithm produced R^2 value of 97%, which was in agreement with the results obtained in the current study. Hassen & Asmare (2019) reported that the ANN algorithm produced R^2 value of 98.2 and 88.5% for training and testing phases MSE values of 0.007 and 0.057. The results were similar to the results obtained in the current study. Newhart *et al.* (2020) conducted a study on the prediction of peracetic acid disinfection for secondary municipal wastewater treatment using the ANN algorithm. Although the R^2 and MSE values were not revealed,

the conclusion of the study was that ANN algorithm was successful in modelling the data. Other studies that reported similar successful results were Vyas & Kulshrestha (2019), Wei *et al*. (2020), and Bhuvaneswari *et al*. (2020).

3.3. Optimization of the energy consumption model

A single objective optimization function was considered because the only problem to be optimized was energy consumption in the biological aeration unit. The single objective function that has to be minimized is defined in Equation (9).

$$\text{Min}[Y_i(AP, COD, NH_3, AR, T)] \tag{9}$$

where Y_i is the energy consumption model, AP is the aeration period, COD is the chemical oxygen demand concentration, NH_3 is the ammonia concentration, AR is the airflow rate, and T is the temperature in the biological aeration unit. The decision variables in the optimization model were AP, COD, NH_3, AR, and T. The constraints are listed in the following equations:

$$1 \leq AP \leq 2 \tag{10}$$

$$30 \leq COD \leq 75 \tag{11}$$

$$1 \leq NH_3 \leq 3 \tag{12}$$

$$1 \leq AR \leq 5 \tag{13}$$

$$32.5 \leq T^{\circ}C \leq 35 \tag{14}$$

The PSO algorithm was successful in minimizing the objective function in order to find the global optimum solution (lowest energy consumption) subject to constraints. The objective function optimum value results from the PSO algorithm are presented in Figure 9. The PSO algorithm converged after performing 199 iterations. Beyond 199 iterations, the algorithm maintained the same solution until 300 iterations were reached and the algorithm terminated as shown in Figure 9.

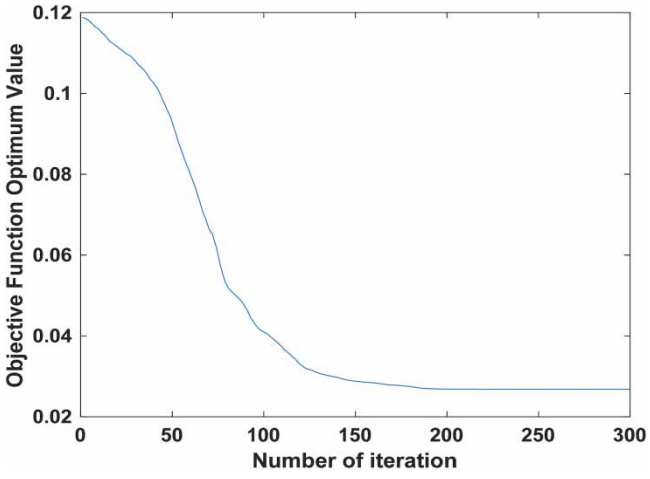

Figure 9 | Optimum objective function value.

The PSO algorithm produced a global optimum solution (objective function optimum value) of 0.0268 kWh after performing 199 iterations as shown in Figure 9. The volume of wastewater treated per cycle was 27 l (0.027 m³). Therefore, the global optimum solution becomes 0.993 kWh/m³, when expressed in terms of the volume of wastewater treated. The optimum measured energy consumption during COD and ammonia removal in the laboratory experiments was 1.611 kWh/m³. The optimum optimized energy consumption during COD and ammonia removal was 0.993 kWh/m³. The percentage reduction between the optimum observed and the

optimum optimized energy consumption during COD and ammonia removal was 38.4%. This is a satisfactory reduction in energy consumption. The results obtained in this study were superior compared with results reported by other scholars (Kusiak & Wei 2013; Asadi *et al.* 2017; Chiavola *et al.* 2017; Han *et al.* 2018; Huang *et al.* 2019; Lu *et al.* 2021). Asadi *et al.* (2017) reported a reduction of 31% in energy consumption. Chiavola *et al.* (2017) reported a reduction of 13% in energy consumption. Kusiak & Wei (2013) reported a reduction of 15% in energy consumption. Huang *et al.* (2019) reported a reduction of 17% in energy consumption. Lu *et al.* (2021) reported a reduction of 7.5% in energy. Han *et al.* (2018) reported a 10% decrease in energy consumption. This indicates that the addition of temperature as a decision variable leads to superior results.

3.4. Sensitivity analysis

Figure 10 presents the results of the sensitivity analysis of the optimized energy consumption model. Aeration period contributed 81% towards energy consumption in the biological aeration unit. This was because when aeration is maintained for 4 h, air pumps/blowers are kept operating in order to supply oxygen for the respiration of microorganisms. If the aeration period is reduced by 50%, plant managers/operators will achieve low energy consumption in the biological aeration unit. The second highest contributor to energy consumption in the biological aeration unit was temperature (10.7%). Temperature controls COD and ammonia removal efficiency, which means that if the temperature is conducive to allow the growth and improve the metabolic rate of microorganisms, rapid removal of COD and ammonia will take place. This will result in less aeration period and airflow supply being required, therefore low energy consumption will be achieved. The airflow rate (4.2%) was the third highest contributor to energy consumption in the biological aeration unit. Airflow supply consumes energy because of the air pumps/blowers utilized. The air pumps/blowers operate 24 h nonstop in order to maintain DO concentration in the wastewater for the respiration and survival of microorganisms. The air pumps/blowers are forced to operate 24 h nonstop because oxygen is partially soluble in wastewater. The low solubility of oxygen in wastewater is caused by the gas–liquid film that prevents gas from dissolving in a liquid as defined by the two-film theory (Lewis & Whitman 1924).

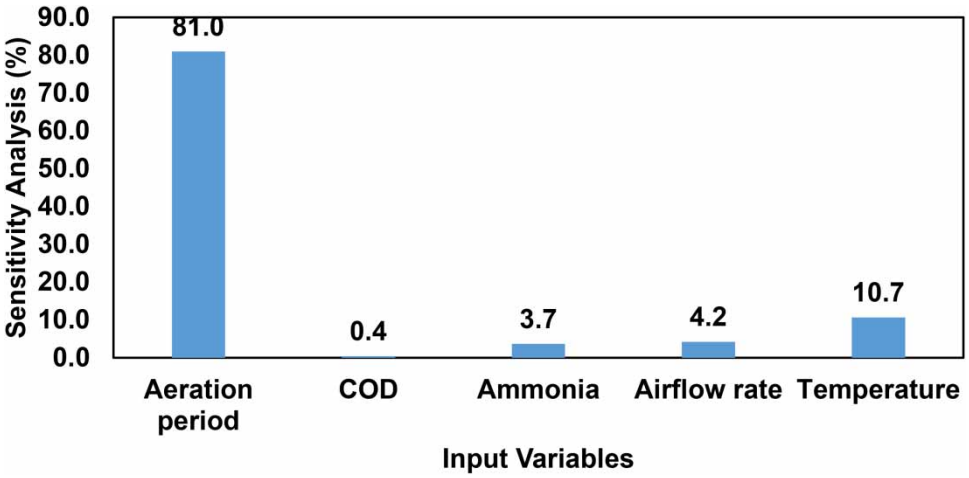

Figure 10 | Sensitivity analysis of the optimized energy consumption model.

Ammonia (3.7%) was the fourth contributor towards energy consumption in the biological aeration unit. Ammonia removal consumes energy consumption indirectly in the biological aeration unit. Ammonia removal relies on microorganisms, and microorganisms require oxygen which is supplied using air pumps/blowers in the biological aeration unit (Ata *et al.* 2017; Mousavi *et al.* 2018). Hence, the removal of ammonia contributes to energy consumption. Similarly, COD (0.4%) removal contributed to energy consumption in the biological aeration unit. Energy consumption during COD removal is consumed similar to ammonia removal in the biological aeration unit (Jungles *et al.* 2017; Fajri *et al.* 2018). However, ammonia removal contributed 3.3% more to energy consumption than COD removal in the biological aeration unit. This is because the removal of ammonia is slow compared with COD removal due to the dominance that heterotrophic bacteria have on autotrophic bacteria

responsible for ammonia removal (Pan *et al.* 2017). Because of this dominance, ammonia removal will require more airflow supply in order to maintain a high DO concentration that can accommodate autotrophic bacteria. In addition, the dominance of heterotrophic bacteria results in a slow removal of ammonia, therefore longer aeration period will be required, which results in high energy consumption.

The relationship between each decision variable and the energy consumption is presented in Figure 11(a)–11(e). The relationship between decision variables (aeration period, COD, ammonia, and airflow rate) increased with an increase in energy consumption. The decision variable that produced the highest positive linear regression was the aeration period (0.0409 kWh) as shown in Figure 11(a). This justifies the fact that the aeration period contributed 81% of energy consumption in the biological aeration unit. This indicates that when the aeration period was extended by 2 h, energy consumption increased by 0.034 kWh in the biological aeration unit.

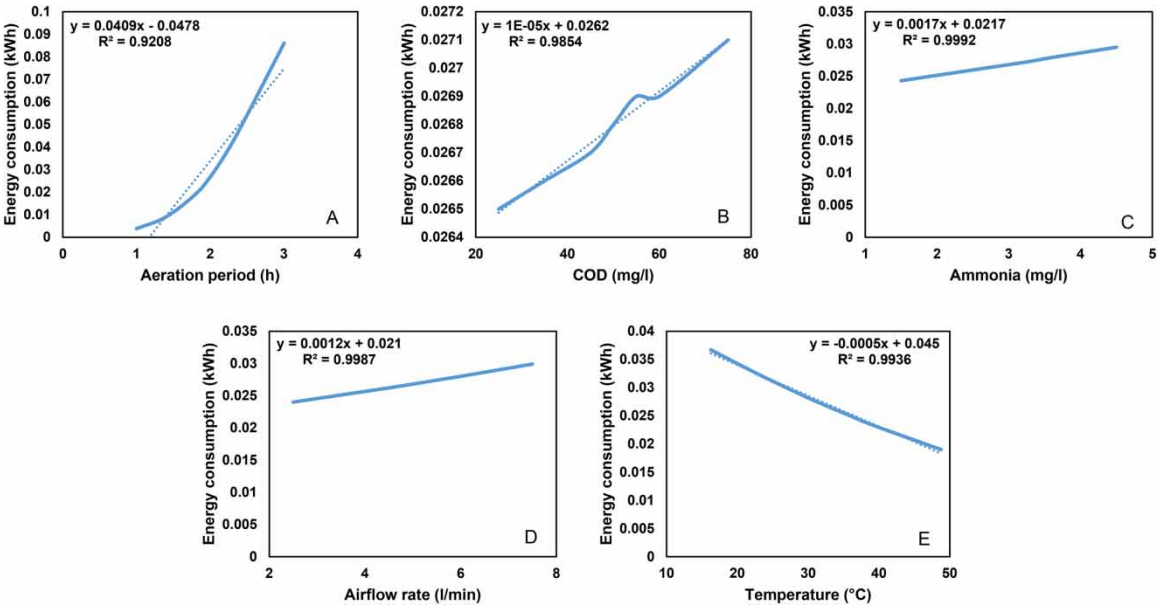

Figure 11 | (a) Effect of aeration period, (b) COD concentration, (c) ammonia concentration, (d) airflow rate, and (e) temperature on energy consumption.

COD and ammonia removal produced a positive linear regression of 0.00005 and 0.0017 kWh as shown in Figure 11(b) and 11(c), respectively. The rate of change in energy consumption caused by the change in ammonia removal (0.0017 kWh) was higher compared with COD removal (0.00005 kWh) in the biological aeration unit. This justifies the fact that ammonia removal requires more oxygen compared with COD removal due to the dominance of heterotrophic bacteria on autotrophic bacteria. Hence ammonia removal consumes high energy compared with COD removal. In addition, high concentrations of ammonia contain high concentrations of free ammonia (Qian *et al.* 2017; Liu *et al.* 2019). Free Ammonia is caused by the presence of ammonia in wastewater, in alkaline conditions. Ammonia concentration of 30 mg/l contains free ammonia in the range between 0.14 and 1.38 mg/l, which slows down the removal of ammonia, resulting in high energy consumption (McCarty 2018).

The relationship between energy consumption and airflow rate produced a positive linear regression of 0.0012 kWh as shown in Figure 11(d). This was lower compared with the aeration period (0.0409 kWh), which justifies the fact that the aeration period contributes more towards energy consumption. Increasing the aeration period by 2 h increases energy consumption by 0.034 kWh, whereas increasing the airflow rate by 5 l/min increased energy consumption by 0.027 kWh. This indicates that low energy consumption can be achieved by reducing the aeration period rather than optimizing airflow rates (Huang *et al.* 2019; Lu *et al.* 2021). Temperature was the only decision variable that produced a negative linear regression of 0.0005 kWh. This means that 0.0425 kWh of energy is reduced when the temperature is increased by 5 °C. This means that energy consumption can be reduced by increasing the temperature of wastewater. Increasing the temperature

in the biological aeration unit increases the removal efficiency of COD and ammonia, resulting in less aeration period, therefore low energy will be consumed. Optimization of the biological aeration unit should be performed at optimum temperatures in order to achieve optimum results (low energy consumption).

Figure 12 shows the results of the observed and optimized energy consumption data points (120) plotted on the same axis. The results in Figure 12 justify the reduction in energy consumption from the optimized energy consumption model. The optimized energy consumption data points were lower than the observed. This indicates that the PSO algorithm was successful in optimizing energy consumption in the biological aeration unit. Table 6 shows the sum of the observed (12.281 kWh) and optimized (10.241 kWh) data. This indicates that the optimized energy consumption data were lower compared with the observed data. The average optimized energy consumption of 0.085 kWh was also lower compared with the average observed energy consumption of 0.102 kWh. The F critical value of 3.881 was lower than the F statistic value of 10.241, which implies that there was a significant difference between the observed and optimized energy consumption. The *P*-value of 0.0017 was less than the significance level of 0.05, which means that there was a significant difference between the optimized and observed energy consumption data. Therefore, the inclusion of the optimum temperature in the optimization problem benefitted the reduction in energy consumption.

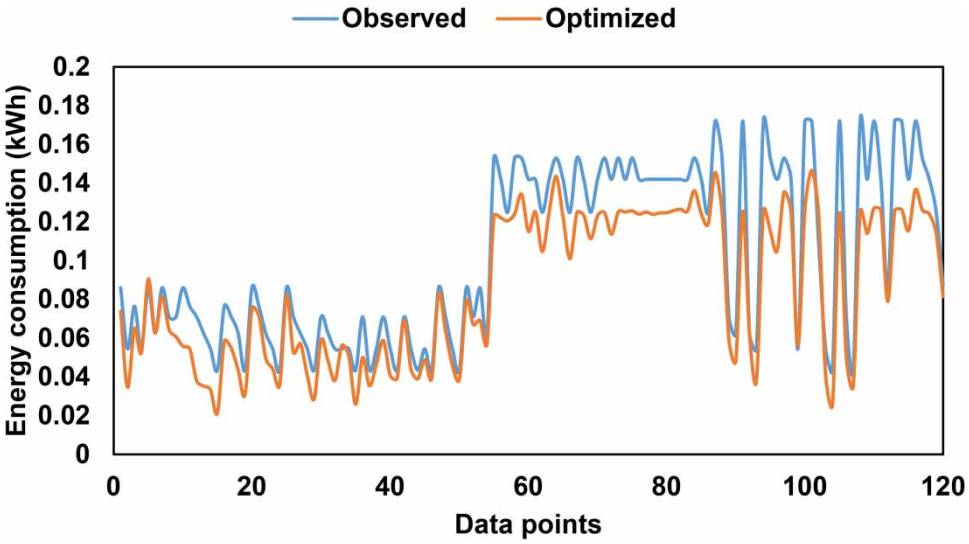

Figure 12 | Observed and optimized energy consumption data points.

Table 6 | The ANOVA test on observed and optimized data set

SUMMARY

Groups	Count	Sum	Average	Variance		
Observed energy	120	12.281	0.102	0.002		
Optimized energy	120	10.241	0.085	0.0015		
ANOVA						
Source of variation	**SS**	**df**	**MS**	**F statistic**	***P*-value**	**F critical**
Between groups	0.017	1	0.017	10.031	0.0017	3.881
Within groups	0.411	238	0.002			
Total	0.429	239				

The robustness of the PSO algorithm in wastewater treatment applications has been reported by a number of authors such as (Nassef *et al*. 2019; Ye *et al*. 2019; Rafati *et al*. 2020; Sinwar *et al*. 2021). Rafati *et al*. (2020)

conducted a study on determining the most effective process control parameter on the activated sludge using the PSO algorithm. The PSO algorithm was successful in optimizing the wastewater parameters in the activated sludge. The control parameters such as COD improved by 1.5%, TSS improved by 1.5%, TN improved by 1.6%, and BOD improved by 2.5%. Ye *et al.* (2019) conducted a study on multi-agent hybrid PSO for wastewater network planning. The PSO algorithm was successful in the optimization planning. The PSO algorithm achieved a 20.13% improvement from the original wastewater treatment scenario. Nassef *et al.* (2019) conducted a study to enhance lipid extraction from microalgae in wastewater treatment using the PSO algorithm. The PSO algorithm was successful in maximizing the lipid extraction of microalgae. The PSO algorithm achieved a 22% increase in lipid extraction when compared with the obtained experimental data. Sinwar *et al.* (2021) conducted a study on the availability and performance optimization of the physical processing unit in a sewage treatment plant using GA and PSO algorithms. The PSO algorithm achieved 99.19% system availability and performance when compared with GA. Yousefi *et al.* (2017) conducted a study on the conjunctive use of wastewater and groundwater in varamin plain. The PSO algorithm was successful in improving the net benefit of cropping pattern optimization. The PSO algorithm achieved an improvement of 35 and 88% for wastewater withdrawals and fertilizer consumption, respectively. Mosayebi & Bahrami (2018) conducted a study on parameter estimation of a biological system using the PSO algorithm. The PSO algorithm was successful and achieved a net improvement of 54.4 and 26.7%. Asadi *et al.* (2017) conducted a study on wastewater treatment aeration process optimization using the PSO algorithm. The PSO algorithm was successful and achieved an energy reduction of 31.4%. Other authors that used the PSO algorithm in wastewater treatment were (Sendrescu 2013; Khoja *et al.* 2018; Faia *et al.* 2019; Kaddoura & Zayed 2019; Lu *et al.* 2021).

4. CONCLUSION

In conclusion, the PSO algorithm managed to reduce energy consumption in the biological aeration unit. The optimized energy consumption was 0.933 kWh/m³ compared with the measured laboratory energy consumption of 1.611 kWh/m³. The total energy consumption reduction was 38.4%, which was superior compared with what other scholars achieved. The aeration period, airflow rate, ammonia removal, and COD removal increased with an increase in energy consumption. The aeration period was the highest contributor (81%) towards energy consumption in the biological aeration unit. This was because during the aeration process, air pumps/blowers are utilized and if aeration is maintained constantly, energy is continuously consumed. The airflow rate was the second highest contributor (4.2%) towards energy consumption. This was because oxygen is partially soluble in wastewater, hence air pumps/blowers operate 24 h nonstop, to try and force oxygen to dissolve in wastewater for the respiration of microorganisms. Ammonia removal (3.7%) contributed more towards energy consumption compared with COD removal (0.4%). Ammonia removal requires a high airflow supply in order to maintain a high DO concentration for autotrophic bacteria to survive. This was caused by the dominance of heterotrophic bacteria on autotrophic bacteria. Temperature played a vital role in energy consumption reduction in the biological aeration unit. Temperature influences the rapid removal of COD and ammonia, which reduces the aeration period and airflow supply required, resulting in low energy consumption. Input parameters that should be considered in optimizing energy consumption are aeration period, airflow rate, ammonia, and temperature since they contributed more towards energy consumption. COD should be eliminated since it only contributed 0.4% of energy consumption in the biological aeration unit.

DATA AVAILABILITY STATEMENT

All relevant data are included in the paper or its Supplementary Information.

CONFLICT OF INTEREST

The authors declare there is no conflict.

REFERENCES

Alisawi, H. A. O. 2020 Performance of wastewater treatment during variable temperature. *Applied Water Science* **10**(4), 1–6. https://doi.org/10.1007/s13201-020-1171-x.

Amiri, R., Ahmadi, M. & Piri, H. 2020 The effects of temperature, mixed liquor suspended solids and velocity on the removal of organic pollutants and kinetic modelling in wastewater sewer systems. *International Journal of Environmental Analytical Chemistry*, 1–15. https://doi.org/10.1080/03067319.2020.1730340.

American Public Health Association (APHA), American Water Works Association, Water Environment Federation. (2012). *Standard methods for the examination of water and wastewater* (22nd ed.). Washington, D.C.: American Public Health Association.

Asadi, A., Verma, A., Yang, K. & Mejabi, B. 2017 Wastewater treatment aeration process optimization: a data mining approach. *Journal of Environmental Management* **203**, 630–639. https://doi.org/10.1016/j.jenvman.2016.07.047.

Ata, O. N., Kanca, A., Demir, Z. & Yigit, V. 2017 Optimization of ammonia removal from aqueous solution by microwave-assisted air stripping. *Water, Air, & Soil Pollution* **228**(11), 448.

Balku, Ş. 2018 Influence of temperature on activated sludge systems. *Celal Bayar University Journal of Science* **14**(1), 77–80. https://doi.org/10.18466/cbayarfbe.357348.

Baquero-Rodríguez, G. A., Martínez, S., Acuña, J., Nolasco, D. & Rosso, D. 2022 How elevation dictates technology selection in biological wastewater treatment. *Journal of Environmental Management* **307**, 114588. https://doi.org/10.1016/j.jenvman.2022.114588.

Bekkari, N. & Zeddouri, A. 2019 Using artificial neural network for predicting and controlling the effluent chemical oxygen demand in wastewater treatment plant. *Management of Environmental Quality: An International Journal*. https://doi.org/10.1108/MEQ-04-2018-0084.

Bhargava, A. 2016 Activated sludge treatment process-concept and system design. *International Journal of Engineering Development and Research* **4**(2), 890–896.

Bhuvaneswari, A., Asha, B., Anbazhagan, S. & Venkatraj, S. 2020 Artificial neural network based prediction of biogas generation through wastewater treatment using anaerobic baffled reactor. *Solid State Technology* **63**(6), 23788–23796.

Brandam, C., Castro-Martínez, C., Délia, M. L., Ramón-Portugal, F. & Strehaiano, P. 2008 Effect of temperature on Brettanomyces bruxellensis: metabolic and kinetic aspects. *Canadian Journal of Microbiology* **54**(1), 11–18. https://doi.org/10.1139/W07-126.

Brehar, M. A., Varhelyi, M., Cristea, V. M., Cristiu, D. & Agachi, S. P. 2019 Influent temperature effects on the activated sludge process at a municipal wastewater treatment plant. *Studia Universitatis Babes-Bolyai Chemia* **64**. doi:10.24193/subbchem.2019.1.09.

Chakawa, S. & Aziz, M. 2021 Investigating the result of current density, temperature, and electrolyte concentration on COD: subtraction of petroleum refinery wastewater using response surface methodology. *Water* **13**(6), 835.

Chapra, S. C., Camacho, L. A. & McBride, G. B. 2021 Impact of global warming on dissolved oxygen and BOD assimilative capacity of the world's rivers: modeling analysis. *Water* **13**(17), 2408. https://doi.org/10.3390/w13172408.

Chiavola, A., Romano, R., Bongirolami, S. & Giulioli, S. 2017 Optimization of energy consumption in the biological reactor of a wastewater treatment plant by means of oxy fuzzy and oxy reduction potential control. *Water, Air, & Soil Pollution* **228**(8), 277. https://doi.org/10.1007/s11270-017-3462-x.

Christoforidou, P., Bariamis, G., Iosifidou, M., Nikolaidou, E. & Samaras, P. 2020 Energy benchmarking and optimization of wastewater treatment plants in Greece. In: *Environmental Sciences Proceedings*. (Vol. 2, No. 1, p. 36). Multidisciplinary Digital Publishing Institute. https://doi.org/10.3390/environsciproc2020002036.

Crini, G. & Lichtfouse, E. 2019 Advantages and disadvantages of techniques used for wastewater treatment. *Environmental Chemistry Letters* **17**(1), 145–155.

Dai, Q., Kelly, J. C., Gaines, L. & Wang, M. 2019 Life cycle analysis of lithium-ion batteries for automotive applications. *Batteries* **5**(2), 48. https://doi.org/10.3390/batteries5020048.

Demir, S. 2020 Artificial neural network simulation of advanced biological wastewater treatment plant performance. *Sigma Journal of Engineering and Natural Sciences* **38**(4), 1713–1728. Available from: https://eds.yildiz.edu.tr/sigma/.

Drewnowski, J., Remiszewska-Skwarek, A., Duda, S. & Łagód, G. 2019 Aeration process in bioreactors as the main energy consumer in a wastewater treatment plant. review of solutions and methods of process optimization. *Processes* **7**(5), 311. https://doi.org/10.3390/pr7050311.

Faia, R., Faria, P., Vale, Z. & Spinola, J. 2019 Demand response optimization using particle swarm algorithm considering optimum battery energy storage schedule in a residential house. *Energies* **12**(9), 1645. https://doi.org/10.3390/en12091645.

Fajri, J. A., Fujisawa, T., Trianda, Y., Ishiguro, Y., Cui, G., Li, F. & Yamada, T. 2018 Effect of aeration rates on removals of organic carbon and nitrogen in small onsite wastewater treatment system (Johkasou). In: *MATEC Web of Conferences*. (Vol. 147, p. 04008). EDP Sciences.

Güçlü, D. & Dursun, Ş. 2010 Artificial neural network modelling of a large-scale wastewater treatment plant operation. *Bioprocess and Biosystems Engineering* **33**(9), 1051–1058. https://doi.org/10.1007/s00449-010-0430-x.

Guerrini, A., Romano, G. & Indipendenza, A. 2017 Energy efficiency drivers in wastewater treatment plants: a double bootstrap DEA analysis. *Sustainability* **9**(7), 1126.

Haberl-Meglič, S., Levičnik, E., Luengo, E., Raso, J. & Miklavčič, D. 2016 The effect of temperature and bacterial growth phase on protein extraction by means of electroporation. *Bioelectrochemistry* **112**, 77–82. https://doi.org/10.1016/j.bioelechem.2016.08.002.

Hamada, M., Adel Zaqoot, H. & Abu Jreiban, A. 2018 Application of artificial neural networks for the prediction of Gaza wastewater treatment plant performance-Gaza strip. *Journal of Applied Research in Water and Wastewater* **5**(1), 399–406.

Han, H. G., Wu, X. L., Zhang, L. & Qiao, J. F. 2018 Intelligent modeling approach to predict effluent quality of wastewater treatment process. *Wastewater and Water Quality* **91**.

Hassen, E. B. & Asmare, A. M. 2019 *Modeling and Monitoring of Treated Wastewater Based on Water Quality Assurance Parameters*.

Huang, S., Zhang, L., Guo, H., Chen, P., Xia, W. & Hu, C. 2019 Modeling and optimization of the activated sludge process. In: *2019 Chinese Control Conference (CCC)*. IEEE. pp. 6481–6486. doi:10.23919/ChiCC.2019.8866516.

Jasim, N. A. 2020 The design for wastewater treatment plant (WWTP) with GPS X modelling. *Cogent Engineering* **7**(1), 1723782.

Jiang, J., Feng, X., Duan, M. & Zhang, Z. 2018 Energy consumption optimization of a synthetic ammonia process based on oxygen purity. *Chemical Engineering Transactions* **70**, 481–486. https://doi.org/10.3303/CET1870081.

Jungles, M. K., Val del Río, Á., Mosquera-Corral, A., Campos, J. L., Méndez, R. & Costa, R. H. 2017 Effects of inoculum type and aeration flowrate on the performance of aerobic granular SBRs. *Processes* **5**(3), 41.

Kaddoura, K. & Zayed, T. 2019 *The Application of Particle Swarm Optimization in Sewer Budget Allocation*. Available from: http://hdl.handle.net/10397/88014.

Kanaujiya, D. K., Paul, T., Sinharoy, A. & Pakshirajan, K. 2019 Biological treatment processes for the removal of organic micropollutants from wastewater: a review. *Current Pollution Reports* **5**(3), 112–128.

Khoja, I., Ladhari, T., Sakly, A. & M'sahli, F. 2018 Parameter identification of an activated sludge wastewater treatment process based on particle swarm optimization method. *Mathematical Problems in Engineering* **2018**. https://doi.org/10.1155/2018/7823930.

Kusiak, A. & Wei, X. 2013 Optimization of the activated sludge process. *Journal of Energy Engineering* **139**(1), 12–17. https://doi.org/10.1061/(ASCE)EY.1943-7897.0000092.

Lewis, W. K. & Whitman, W. G. 1924 Principles of gas absorption. *Industrial & Engineering Chemistry* **16**(12), 1215–1220.

Li, W., Li, L. & Qiu, G. 2017 Energy consumption and economic cost of typical wastewater treatment systems in Shenzhen, China. *Journal of Cleaner Production* **163**, S374–S378. https://doi.org/10.1016/j.jclepro.2015.12.109.

Liu, Y., Ngo, H. H., Guo, W., Peng, L., Wang, D. & Ni, B. 2019 The roles of free ammonia (FA) in biological wastewater treatment processes: a review. *Environment International* **123**, 10–19.

Loutfi, H., Pellen, F., Le Jeune, B., Lteif, R., Kallassy, M., Le Brun, G. & Abboud, M. 2020 Real-time monitoring of bacterial growth kinetics in suspensions using laser speckle imaging. *Scientific Reports* **10**(1), 1–10.

Lu, L., Zheng, H., Jie, J., Zhang, M. & Dai, R. 2021 Reinforcement learning-based particle swarm optimization for sewage treatment control. *Complex & Intelligent Systems* **7**(5), 2199–2210. https://doi.org/10.1007/s40747-021-00395-w.

Marlina, E., Purwanto, P. & Sudarno, S. 2021 COD removal, decolorization, and energy consumption of electrocoagulation as a wastewater treatment process. In: *IOP Conference Series: Earth and Environmental Science*. (Vol. 896, No. 1, p. 012043). IOP Publishing. doi:10.1088/1755-1315/896/1/012043.

McCarty, P. L. 2018 What is the best biological process for nitrogen removal: when and why? *Environmental Science & Technology* **52**(7), 3835–3841.

Menegol, T., Diprat, A. B., Rodrigues, E. & Rech, R. 2017 Effect of temperature and nitrogen concentration on biomass composition of Heterochlorella luteoviridis. *Food Science and Technology* **37**(SPE), 28–37. https://doi.org/10.1590/1678-457X.13417.

Mosayebi, R. & Bahrami, F. 2018 A modified particle swarm optimization algorithm for parameter estimation of a biological system. *Theoretical Biology and Medical Modelling* **15**(1), 1–10. https://doi.org/10.1186/s12976-018-0089-6.

Mousavi, S. A., Mehralian, M., Khashij, M. & Ibrahim, S. 2018 Effect of air flow rate and C/N ratio on biological nitrogen removal through the CANON process treating reject water. *Environmental Technology* **39**(22), 2891–2899. https://doi.org/10.1080/09593330.2017.1369578.

Murillo, M. 2018 Design of Aeration Tank and Clarifier. A Discussion. *A Discussion. (April 16, 2018)*.

Musvoto, E. & Ikumi, D. 2016 *Energy use Reduction in Biological Nutrient Removal Wastewater Treatment Plants*.

Nassef, A. M., Rezk, H., Abdelkareem, M. A., Alaswad, A. & Olabi, A. 2019 Application of fuzzy modelling and particle swarm optimization to enhance lipid extraction from microalgae. *Sustainable Energy Technologies and Assessments* **35**, 73–79. https://doi.org/10.1016/j.seta.2019.06.003.

Newhart, K. B., Goldman-Torres, J. E., Freedman, D. E., Wisdom, K. B., Hering, A. S. & Cath, T. Y. 2020 Prediction of peracetic acid disinfection performance for secondary municipal wastewater treatment using artificial neural networks. *ACS ES&T Water* **1**(2), 328–338. https://doi.org/10.1021/acsestwater.0c00095.

Ozturk, M. C., Serrat, F. M. & Teymour, F. 2016 Optimization of aeration profiles in the activated sludge process. *Chemical Engineering Science* **139**, 1–14. https://doi.org/10.1016/j.ces.2015.09.007.

Pan, W., Xiong, Y., Huang, Q. & Huang, G. 2017 Removal of nitrogen and COD from reclaimed water during long-term simulated soil aquifer treatment system under different hydraulic conditions. *Water* **9**(10), 786.

Panepinto, D., Fiore, S., Zappone, M., Genon, G. & Meucci, L. 2016 Evaluation of the energy efficiency of a large wastewater treatment plant in Italy. *Applied Energy* **161**, 404–411. https://doi.org/10.1016/j.apenergy.2015.10.027.

Pawlita-Posmyk, M., Wzorek, M. & Płaczek, M. 2018 The influence of temperature on algal biomass growth for biogas production. In *MATEC Web of Conferences*. (Vol. 240, p. 04008). EDP Sciences. https://doi.org/10.1051/matecconf/201824004008.

Qian, W., Peng, Y., Li, X., Zhang, Q. & Ma, B. 2017 The inhibitory effects of free ammonia on ammonia oxidizing bacteria and nitrite oxidizing bacteria under anaerobic condition. *Bioresource Technology* **243**, 1247–1250.

Rafati, M., Pazouki, M., Ghadamian, H., Hossein Nia, A. & Jalilzadeh, A. 2020 Determine the most effective process control parameters on activated sludge based on particle swarm optimisation algorithm (Case study: south wastewater treatment

plant of Tehran). *International Journal of Environmental Analytical Chemistry*, 1–22. https://doi.org/10.1080/03067319.2020.1836169.

Saleh, I. A., Zouari, N. & Al-Ghouti, M. A. 2020 Removal of pesticides from water and wastewater: chemical, physical and biological treatment approaches. *Environmental Technology & Innovation* **19**, 101026.

Sendrescu, D. 2013 Parameter Identification of Anaerobic Wastewater Treatment Bioprocesses Using Particle Swarm Optimization. *Mathematical Problems in Engineering* **2013**, 8 pages, 2013. https://doi.org/10.1155/2013/103748

Sharghi, E., Nourani, V., Ashrafi, A. A. & Gökçekub, H. 2019 Monitoring effluent quality of wastewater treatment plant by clustering based artificial neural network method. *Desalination and Water Treatment* **164**, 86–97.

Shen, S., Wang, G., Zhang, M., Tang, Y., Gu, Y., Jiang, W., Wang, Y. & Zhuang, Y. 2020 Effect of temperature and surfactant on biomass growth and higher-alcohol production during syngas fermentation by Clostridium carboxidivorans P7. *Bioresources and Bioprocessing* **7**(1), 1–13. https://doi.org/10.1186/s40643-020-00344-4.

Siatou, A., Manali, A. & Gikas, P. 2020 Energy consumption and internal distribution in activated sludge wastewater treatment plants of Greece. *Water* **12**(4), 1204. https://doi.org/10.3390/w12041204.

Singh, K. K. 2022 Advance technology in wastewater treatment: a brief assessment. *International Journal of New Chemistry* **9**(3), 361–372.

Singh, P. & Kansal, A. 2018 Energy and GHG accounting for wastewater infrastructure. *Resources, Conservation and Recycling* **128**, 499–507. https://doi.org/10.1016/j.resconrec.2016.07.014.

Sinwar, D., Saini, M., Singh, D., Goyal, D. & Kumar, A. 2021 Availability and performance optimization of physical processing unit in sewage treatment plant using genetic algorithm and particle swarm optimization. *International Journal of System Assurance Engineering and Management* **12**(6), 1235–1246. https://doi.org/10.1007/s13198-021-01163-2.

Stasinakis, A. S., Charalambous, P. & Vyrides, I. 2022 Dairy wastewater management in EU: produced amounts, existing legislation, applied treatment processes and future challenges. *Journal of Environmental Management* **303**, 114152.

Struk-Sokołowska, J., Ofman, P. & Demirel, S. 2019 Artificial neural network (ANN) approach for modeling of selected biogenic compounds in a mixture of treated municipal and dairy wastewater. In: *E3S Web of Conferences*. (Vol. 100, p. 00077). EDP Sciences. https://doi.org/10.1051/e3sconf/201910000077.

Van Vuuren, L. 2013 Of watts and drops-new compendium switches on the lights for SA energy efficiency in water: water and energy. *Water Wheel* **12**(5), 13–15. Available from: https://hdl.handle.net/10520/EJC142548

Vogelaar, J. C. T., Klapwijk, A., Van Lier, J. B. & Rulkens, W. H. 2000 Temperature effects on the oxygen transfer rate between 20 and 55 C. *Water Research* **34**(3), 1037–1041. https://doi.org/10.1016/S0043-1354(99)00217-1.

Vyas, M. & Kulshrestha, M. 2019 Artificial neural networks for forecasting wastewater parameters of a common effluent treatment plant. *International Journal of Environment and Waste Management* **24**(3), 313–336. Available from: https://www.inderscienceonline.com/doi/epdf/10.1504/IJEWM.2019.103106.

Wakeel, M., Chen, B., Hayat, T., Alsaedi, A. & Ahmad, B. 2016 Energy consumption for water use cycles in different countries: a review. *Applied Energy* **178**, 868–885. https://doi.org/10.1016/j.apenergy.2016.06.114.

Wei, W., Haas, C. N. & Farouk, B. 2020 Development of a CFD-based artificial neural network metamodel in a wastewater disinfection process with peracetic acid. *Journal of Environmental Engineering* **146**(12), 04020140. Available from: https://ascelibrary.org/doi/abs/10.1061/%28ASCE%29EE.1943-7870.0001822.

Winter, D. 2011 *Power Outages and Their Impact on SA's Water and Wastewater Sectors*. Water Research Commission.

Ye, X., Chen, B., Jing, L., Zhang, B. & Liu, Y. 2019 Multi-agent hybrid particle swarm optimization (MAHPSO) for wastewater treatment network planning. *Journal of Environmental Management* **234**, 525–536. https://doi.org/10.1016/j.jenvman.2019.01.023.

Yousefi, M., Banihabib, M. E., Soltani, J. & Rouzbahani, A. 2017 Non-Linear programming and particle swarm optimization model for management of conjunctive use of wastewater and groundwater in Varamin Plain. doi:10.22092/JWRA.2017.113678.

Zeraik, A. E. & Nitschke, M. 2012 Influence of growth media and temperature on bacterial adhesion to polystyrene surfaces. *Brazilian Archives of Biology and Technology* **55**, 569–576.

Zhang, Q., Chen, X., Luo, W., Wu, H., Liu, X., Chen, W., Tang, J. & Zhang, L. 2019 Effects of temperature on the characteristics of nitrogen removal and microbial community in post solid-phase denitrification biofilter process. *International Journal of Environmental Research and Public Health* **16**(22), 4466.

Zou, L., Li, H., Wang, S., Zheng, K., Wang, Y., Du, G. & Li, J. 2019 Characteristic and correlation analysis of influent and energy consumption of wastewater treatment plants in Taihu Basin. *Frontiers of Environmental Science & Engineering* **13**(6), 1–14. https://doi.org/10.1007/s11783-019-1167-7.

Żyłka, R., Karolinczak, B. & Dąbrowski, W. 2021 Structure and indicators of electric energy consumption in dairy wastewater treatment plant. *Science of the Total Environment* **782**, 146599. https://doi.org/10.1016/j.scitotenv.2021.146599.

First received 2 August 2022; accepted in revised form 23 November 2022. Available online 6 December 2022